ELSEVIER

Journal of Nuclear Materials 299 (2001) 32–42

journal of nuclear materials

www.elsevier.com/locate/jnucmat

Behavior of plutonium and americium at liquid cadmium cathode in molten LiCl–KCl electrolyte

Masatoshi Iizuka [a,*], Koich Uozumi [a], Tadashi Inoue [a], Takashi Iwai [b], Osamu Shirai [b], Yasuo Arai [b]

[a] *Nuclear Fuel Cycle Department, Central Research Institute of Electric Power Industry, Iwato-kita 2-11-1, Komae-shi, Tokyo 201-8511, Japan*

[b] *Japan Atomic Energy Research Institute, Oarai, Higashi-Ibaraki, Ibaraki 311-1394, Japan*

Received 8 March 2001; accepted 28 July 2001

Abstract

The effects of the electrochemical conditions on the behavior of plutonium and proper conditions for plutonium recovery at the liquid cadmium cathode (LCC) used in the pyrometallurgical reprocessing were studied by the electrotransport experiments with small, not stirred electrodes. Plutonium was successfully collected up to 7.75 wt% without disturbance by solid phase formation at the surface. Plutonium collected beyond saturation formed intermetallic compound $PuCd_6$ and accumulated at the bottom of the LCC. The cathodic current density adequate for plutonium collection was proportional to the concentration of plutonium in the molten salt. The behavior of americium was reasonably explained by a local equilibrium model between plutonium and americium at the surface of the LCC, although thermodynamic study and quantitative analysis are needed for further understanding. The plutonium collection rate in practical electrorefiner was estimated to be 324 g/h for one LCC by extrapolation of the experimental results.

PACS: 28.41.Bm; 81.15.Pq; 82.65.Dp; 82.80.Fk

1. Introduction

Metallic fuel cycle which consists of the metal (U–Zr or U–Pu–Zr) fueled fast reactor and the pyrometallurgical reprocessing has been proposed originally by Argonne National Laboratory (ANL) as an innovative nuclear fuel cycle technology [1]. The metallic fuel cycle has an excellent safety feature originating from high thermal conductivity of the metal fuel [2]. It also has economic advantage because the pyrometallurgical reprocessing plant is estimated to be smaller than conventional aqueous reprocessing plants due to the fewer steps and the more compact equipments [3].

The main step in the pyrometallurgical process is the molten salt electrorefining [4], where the most part of the actinide elements are recovered and decontaminated from the fission products. Fig. 1 shows a schematic flow of the normal operation of the electrorefining step. The spent fuel is cut into small pieces, loaded in a steel basket, and immersed into molten chloride electrolyte. Almost all of the actinide elements in the spent fuel are anodically dissolved. The noble metal fission products are left in the anode basket by controlling the anode potential because they are less stable as chlorides than the actinide elements. The chemically active fission products such as alkali, alkaline earth, and rare-earth metals exchange with the actinide chlorides in the electrolyte and accumulate in the form of chlorides. Two kinds of cathodes are used to obtain different streams of products. One is a solid cathode made of iron for the blanket material production, and the other is a liquid cadmium cathode (LCC) for the driver fuel material

* Corresponding author. Tel.: +81-3 3480 2111; fax: +81-3 3480 7956.

E-mail address: iizuka@criepi.denken.or.jp (M. Iizuka).

0022-3115/01/$ - see front matter
PII: S0022-3115(01)00667-5

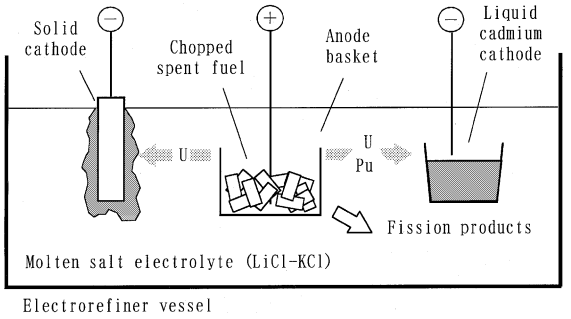

Fig. 1. Schematic flow of routine operation of the electrorefining step.

production. The free energy changes of chloride formation for some actinide and lanthanide elements at the two types of cathodes are shown in Fig. 2 [5]. At the solid cathode, uranium is selectively collected because the free energy change of chloride formation for uranium differs more than 30 kJ/mol from those for the other actinide and lanthanide elements. On the other hand, the free energy changes of the actinide elements are close to each other at the LCC as seen in Fig. 2 because the transuranium elements (plutonium, neptunium, americium and curium) are stabilized in the LCC due to their very low activity coefficients in liquid cadmium [6,7]. Therefore, transuranium elements can be collected at the LCC together with uranium. Although a small amount of lanthanide fission products comes into the LCC product as expected from Fig. 2, it does not impact the performance of the fuel fabrication process or the reactor loaded with recycled fuel [8,9]. The inevitable coexistence of γ-emitting lanthanide fission products in recycled fuel could be rather an advantage in terms of non-proliferation.

The use of the LCC is the most important technology in the pyrometallurgical process because plutonium is recovered and decontaminated from fission products in this step. Since the performance of the LCC significantly

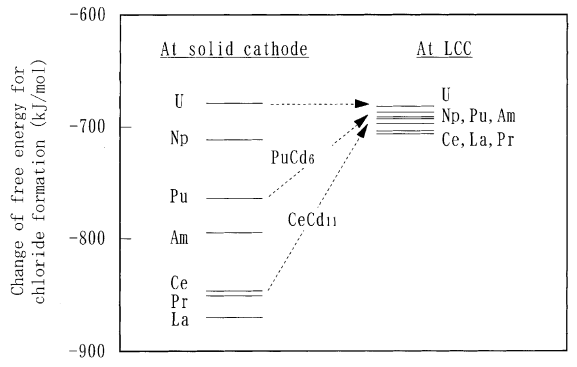

Fig. 2. ΔG_f of several chlorides at solid and liquid cadmium cathodes.

influences the feasibility of the pyrometallurgical reprocessing, ANL studied plutonium recovery with the LCC in depth with the laboratory scale equipment [10–13]. They devised the 'pounder-type' LCC, which has a cylindrically shaped ceramic block rotating and reciprocating vertically above the cathode cadmium [13]. The pounder facilitates exchange of the electrolyte above the cathode and pushes solid product, which hampers stable LCC operation, down into the cathode cadmium. It was reported that more than 15 wt% of plutonium was recovered into 200 to 250 g of cathode cadmium [13] using the pounder-type LCC made of beryllia or aluminum nitride. We have reported on the behavior of uranium at LCCs, especially focusing on the formation of dendritic uranium deposit [14,15]. In those studies, it was shown that stirring in the cathode cadmium with the vertical paddles is effective to restrain growth of the uranium dendrite and that uranium can be collected into the LCCs at the cathodic current density of 0.2 A/cm^2 up to about 10 wt% in the cathode without dendrite formation [15]. In addition to the uranium studies, we have launched a joint research program with Japan Atomic Energy Research Institute (JAERI) on the pyrometallurgical processes. In 1999, a plutonium electrorefining apparatus equipped with a LCC assembly was fabricated and installed. In this study, fundamental plutonium electrotransport experiments were carried out in order to understand the effects of electrochemical conditions on the behavior of plutonium at the LCC preceding investigation of the engineering factors like stirring method.

2. Experiment

2.1. Apparatus

All the experiments were carried out in a high purity argon atmosphere glove box. Both the oxygen and the moisture levels in the atmosphere were kept less than 2 ppm during the tests. Fig. 3 is a schematic view of the experimental apparatus. Inner diameter and depth of the container for the molten salt were 124 and 120 mm, respectively. About 1200 g of lithium chloride–potassium chloride (LiCl–KCl) eutectic mixture was loaded in this container. Under the molten salt electrolyte, a liquid cadmium layer was placed and used as an anode which supplied plutonium in the electrotransport experiments. The amount of the anode cadmium was about 1400 g. The salt and the anode cadmium were heated with an electric furnace and the temperature of the system was kept to 773 ± 1 K by a proportional–integral–differential (PID) controller. The molten salt and the liquid cadmium anode layer were stirred by rotating small vertical paddles (30 mm OD, 6 mm height) at 60 rpm.

The electrorefining apparatus and the cathode assembly were originally designed to accommodate a LCC

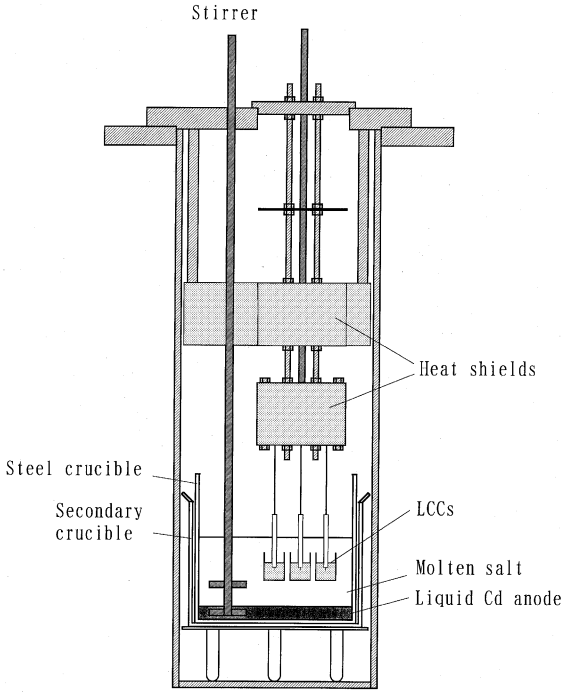

Fig. 3. Schematic view of the experimental apparatus.

of 50 mm outer diameter, which would be stirred to facilitate the mass transfer of plutonium. In this study, however, much smaller cathodes were used because the study aimed to understand the effects of fundamental electrochemical conditions on the behavior of plutonium at the LCC before investigation of the engineering factors like stirring method. The size of the cathode crucible used in this study was 9 mm in diameter and 16 mm in depth. About 3–5 g of cadmium was loaded in the crucible. A tungsten wire of 1 mm diameter with a high purity alumina sheath of 2 mm outer diameter was immersed in the cathode cadmium and was used as an electric lead. It was difficult to determine the surface area of the LCC exactly because it is largely affected by the wetting behavior of liquid cadmium to the alumina parts. In this study, the surface area was evaluated to be 0.605 cm^2 simply on the assumption that the annular region between the cathode crucible and the alumina sheath was flat. A silver–silver chloride (1 wt% AgCl in LiCl–KCl) reference electrode contained in a thin Pyrex glass tube was used. The potential of the reference electrode was very stable at 773 K throughout the experiments.

2.2. Chemicals

The chlorides (LiCl–KCl, $CdCl_2$ and AgCl) were purchased from Anderson Physical Laboratory. Because their purity was no less than 99.99% and their moisture content was negligibly low, they were used without additional purification procedure. Cadmium metal of more than 99.9999% purity for the anode and the cathode was purchased from Rare Metallic Corporation. Because the cadmium had been packed under vacuum just after production to avoid oxidation by the air, it was not washed or polished before use. The purity of the other electrode materials such as tungsten, tantalum, molybdenum and silver, was no less than 99.95%. These metals were polished with #1000 emery paper. They were then washed in diluted nitric acid and in distilled water with an ultrasonic cleaner. PuO_2 used in this study contained about 2% of americium which was generated by (n, γ) reaction of Pu^{239} and β-decay.

2.3. Analytical procedures

EG&G Princeton Applied Research potentio/galvanostat Model 273A and EG&G 270/250 Research Electrochemistry Software were used for both the electrochemical measurement and the constant-current electrotransport. The concentrations of plutonium and cadmium in the molten salt were determined by inductively coupled plasma-atomic emission spectroscopy (ICP-AES) of the samples. The cathode products were analyzed by scanning electron microscope (SEM) and electron probe microanalyzer (EPMA). An X-ray diffractometer (XRD) was also used to determine the chemical form of the cathode deposit.

2.4. Adjustment of plutonium concentrations in molten salt and liquid cadmium anode

In our previous studies on the chemistry and the electrochemistry of plutonium in molten chlorides, plutonium trichloride ($PuCl_3$) was prepared in the following three steps [16]: (a) carbothermic reduction of PuO_2 to produce PuN [17], (b) formation of $PuPt_3$ by reaction between PuN and platinum metal, and (c) exchange reaction between $PuPt_3$ and cadmium chloride ($CdCl_2$) which yields $PuCl_3$ in a LiCl–KCl/liquid cadmium system. Although this is an established method to obtain $PuCl_3$ in LiCl–KCl, a large amount of expensive platinum metal becomes radioactive waste mixed with toxic cadmium. This problem is especially serious when a large amount of $PuCl_3$ is needed. Then, another method was adopted in this study. PuN obtained in the step (a) was loaded in a basket made of molybdenum mesh, then immersed into the molten LiCl–KCl and directly reacted with $CdCl_2$ to produce $PuCl_3$ and N_2 gas. The amounts of PuN and $CdCl_2$ at the beginning of this study were 44.2 and 53.5 g (excess of about 5% over the required amount for complete reaction with PuN), respectively. The molten salt samples and the cyclic voltammograms (CVs) for plutonium in the salt were taken periodically in order to follow the progress of the reaction. The

experiment was finished five days after the beginning of the reaction because the change of CVs became almost negligible. There was a small amount of brown residue at the bottom of the basket, which was presumed to be PuO_2 generated by oxidation of PuN during storage. Fig. 4 shows the change of the concentrations of plutonium and cadmium in the molten salt during that process. It can be seen that the reaction between $PuCl_3$ and $CdCl_2$ was almost completed in 16 h. Although the actual plutonium concentration in the salt was slightly lower than expected, the reaction efficiency was considered nearly 100% taking account of the oxidation of PuN and the error from the chemical analysis of the samples.

The concentration of plutonium in the liquid cadmium anode was adjusted by reduction of $PuCl_3$ in the molten salt phase by addition of cadmium–lithium alloy as a reducing agent. Lithium metal itself was not used to avoid rapid reaction with plutonium chloride and dispersion of fine plutonium metal powder product, resulting in low material balance. As well as in the case of $PuCl_3$ preparation, the molten salt/liquid cadmium anode samples and the CVs for plutonium in the salt were taken periodically. The reaction was considered to complete in 20 h because no more change could be found in the CVs after that. The reaction efficiency in the reduction step was determined to be approximately 100% based on the chemical analysis of the samples.

After all these steps were completed, the concentrations of plutonium in the molten salt and in the liquid cadmium anode were 2.28 and 1.72 wt%, respectively.

3. Results and discussion

3.1. Voltammetric study on the electrochemistry of plutonium at the liquid cadmium electrode

Preceding the electrotransport experiments, CVs were measured with the liquid cadmium electrode in order to obtain primary information about the electrochemical reaction of plutonium at the LCC. Fig. 5 shows the CVs for LiCl–KCl–$PuCl_3$ measured with a liquid cadmium electrode whose dimension is identical to those used in the electrotransport experiments. The surface area of the electrode was estimated from the inner diameter of the crucible and the outer diameter of the insulator tube of the electric lead.

The reduction current of plutonium started to flow at about −1.2 V and it made a bump at about −1.5 V. In a CV measured with a solid electrode shown also in Fig. 5, the peak current for the reduction of plutonium appeared at −1.7 V which is 0.2 V lower than that in the case of the liquid cadmium electrode. The activity coefficient of plutonium in liquid cadmium at 773 K is reported to be 1.4×10^{-4} [6]. Because this value is equivalent to a 197 mV shift to the higher direction for a three-electron reaction at 773 K, the above potential difference between the two kinds of electrodes is thermodynamically reasonable.

In general, the current by diffusion-controlled reactions is proportional to square root of the potential scanning rate in CV [18]. However, the increase of the reduction current of plutonium at the liquid cadmium electrode was very little when the potential scanning rate

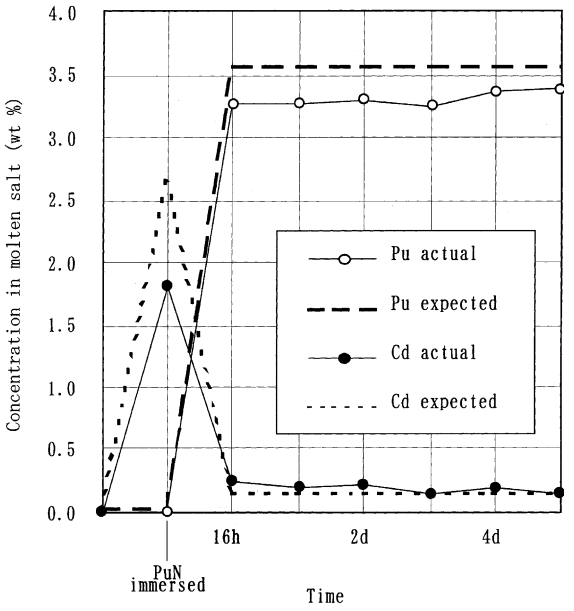

Fig. 4. Change of Pu and Cd concentrations in molten salt during PuCl, preparation from PuN.

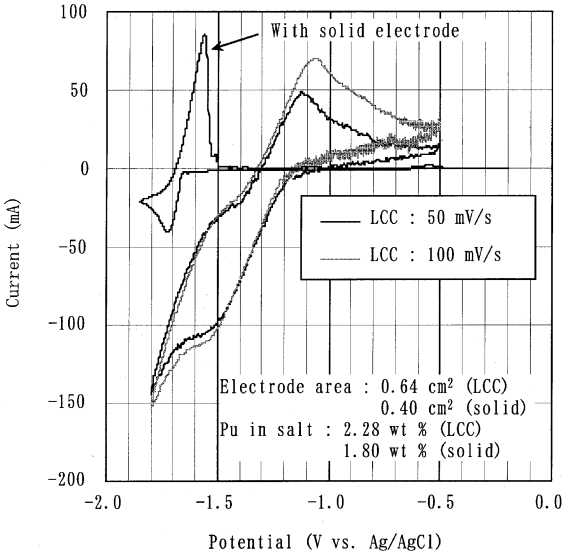

Fig. 5. CVs for Pu in molten LiCl–KCL with solid and liquid cadmium electrodes.

was increased from 50 to 100 mV/s. This behavior indicates that the concentration of plutonium at the surface of the electrode went over its solubility limit and that a solid phase which was supposed to be $PuCd_6$ from the Cd–Pu phase diagram [19] was formed. In such a situation, the supply of free cadmium which lowers the activity of the reduced plutonium would be disturbed by the solid phase barrier. Then the reduction current of plutonium would not depend on the potential scanning rate, and it would be controlled by the supply of free cadmium from the inside to the surface of the electrode. When the potential was turned to the positive direction, the reduction product ought to have accumulated near the surface of the cathode and the oxidation peak current should have been controlled by diffusion of trivalent plutonium ion in the molten salt. Consequently, the oxidation peak current at −1.1 V is approximately in proportion to square root of the potential scanning rate as shown in Fig. 5.

3.2. Plutonium electrotransport experiments at constant cathodic current density

In order to understand the behavior of plutonium at LCC and the proper conditions for plutonium recovery, the electrotransport experiments were carried out at various cathodic current densities and plutonium concentrations in the molten salt. Major results are summarized in Table 1 with the experimental conditions. There was essentially no change in the concentration of plutonium in the molten salt during each test. Because the amount of plutonium transported to the cathodes was very small compared to the inventory in the anode, the change of plutonium concentration in the anode was negligibly small. The polarization of the anode was also very small because the surface area of the anode was about two hundred time larger than that of the cathode.

3.2.1. The change of the LCC potential and the plutonium collection efficiency

Run 1 to 4 were carried out at relatively lower plutonium concentration in the molten salt (2.11–2.34 wt%). The changes of the LCC potential in these tests are shown in Fig. 6. At the cathodic current density of 33–41 mA/cm^2, the cathode potential was kept between −1.4 and −1.55 V after a slight shift to the lower direction at the beginning. In this range of the potential, the reduction of plutonium followed by Pu–Cd intermetallic compound is expected to occur at the LCC from the result of the CV measurement. The moderate change of the cathode potential indicated that plutonium was collected into the LCC without abrupt growth of solid phase at the interface. The collection efficiency for plutonium calculated from the increase of the cathode weight and the total electric charge as shown below were nearly 100% on these conditions.

$$\text{Collection efficiency (\%)} = \frac{\text{Increase of cathode weight (g)} \times 100}{\text{Total electric charge (C)}/1210\ \text{(C/g Pu)}}.$$

This result supports the above consideration about the smooth collection of plutonium. Fig. 7 is the appearance of the cathode cadmium ingot taken out of the crucible in Run 2 where plutonium was collected up to 7.75 wt% into the LCC at the cathodic current density of 41 mA/cm^2. The top of the ingot was round due to the poor wetting between cadmium and the alumina crucible. Although there was a little inequality on the surface of the LCC, no growth of dendritic deposit was found.

In Run 3, the cathode potential went down to −1.65 V at the cathodic current density of 50 mA/cm^2. The solidified salt on the top of the cathode cadmium was white after this run although LiCl–KCl containing about 2 wt% of plutonium is usually light blue. The collection efficiency of plutonium was about 80% in this

Table 1
Conditions and results of the Pu electrotransport experiments with the LCCs

Run no.	Pu concentration in molten (wt%)	Cathodic current density (mA/cm^2)	Electrotransport time (s)	Electricity passed in experiment (C)	Initial amount of cathode (g)	Increase of cathode weight (g)	Collection efficiency (%)	Final Pu concentration in cathode (wt%)
1	2.28	33	12000	240	4.036	1.983	100	4.68
2	2.11	41	11870	297	2.918	0.245	105	7.75
3	2.28	50	7800	234	4.899	0.1555	80.6	3.08
4	2.11	66	6500	260	3.406	0.0023	1.07	0.07
5	4.6	66	7200	288	4.0287	N/A	N/A	N/A
6	4.6	82	5400	270	4.0056	N/A	N/A	N/A
7	4.6	100	5400	324	4.024	N/A	N/A	N/A
8	4.6	132	5400	432	4.082	N/A	N/A	N/A

$$\text{Collection efficiency (\%)} = \frac{\text{Increase of cathode weight (g)} \times 100}{\text{Total electric charge (C)}/1210\text{(C/g Pu)}}.$$

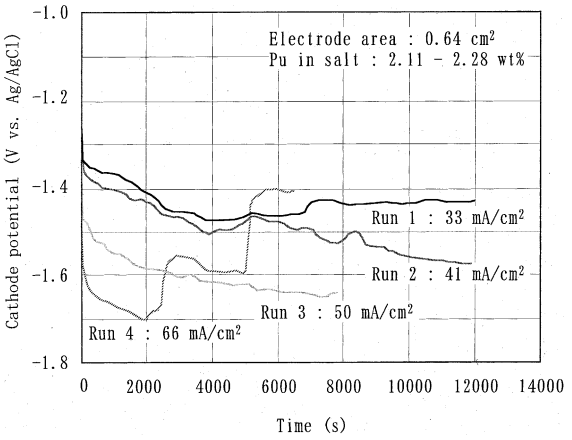

Fig. 6. Change of LCC potential in the Pu electrotransport tests (at the lower Pu concentration in molten salt).

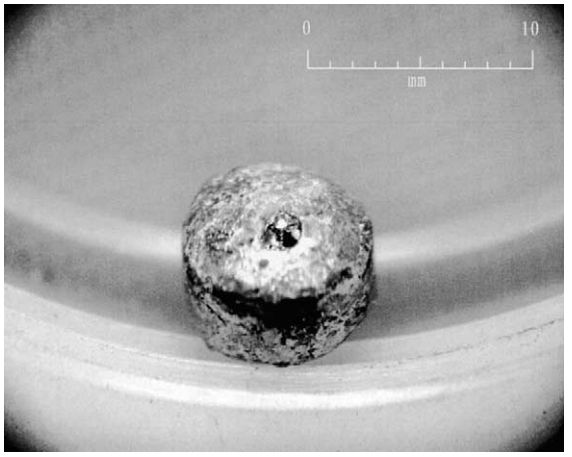

Fig. 7. Cathode Cd ingot obtained after the Pu electrotransport test at the cathodic current density of 41 mA/cm^2.

run, a little lower than in the preceding cases at the lower cathodic current densities. These results indicate that lithium in the electrolyte was electrochemically reduced at the LCC at −1.65 V and that the reduced lithium reacted with plutonium chloride near the cathode after the electrotransport. Lithium forms a very stable chloride whose standard potential is more than 0.6 V lower than that of plutonium at an inert electrode. However, redox potential of lithium is about 0.4 V higher at the LCC due to the very low activity coefficient of plutonium in liquid cadmium ($1.8–2.6 \times 10^{-3}$) [20]. In addition, the concentration of lithium ion around the LCC was very high because it was one of the solvent cations. In that situation, lithium should be reduced at the LCC in competition with plutonium. Fig. 8 shows a CV measured with a liquid cadmium electrode for LiCl–KCl

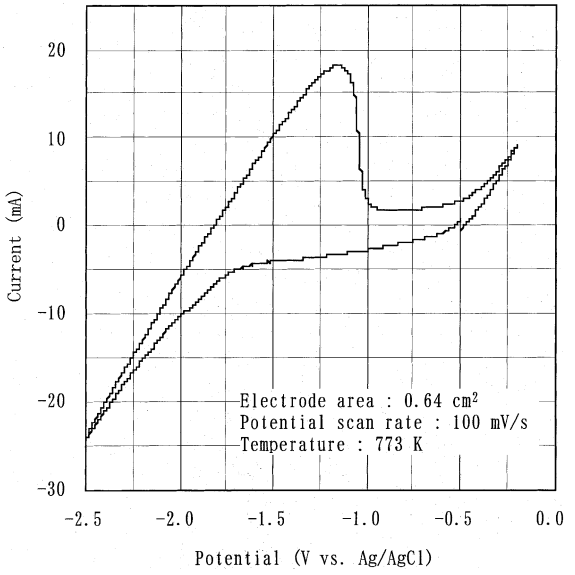

Fig. 8. CVs for blank LiCl–KCL with liquid cadmium electrode.

containing no plutonium. It can be seen that the reduction current of lithium increases from around −1.6 V, suggesting the validity of the above consideration.

When the cathodic current density was increased to 66 mA/cm^2, the cathode potential once descended to −1.7 V and subsequently ascended in two steps. After the experiment, the cathode was visually inspected. The lower part of the alumina insulator sheath of the electric lead for the LCC had turned black and a deposit with metallic gloss was found on that region. X-ray diffraction analysis showed that the major portion of this deposit was $PuCd_6$. At such high cathodic current density, it is expected that the concentration of lithium at the surface of the LCC was so high due to the low cathode potential that the lithium reacted with the alumina sheath. It is very likely that the alumina sheath was wetted much more easily with liquid cadmium due to the reaction with lithium. This is considered the reason why the alumina sheath worked as a thin LCC and $PuCd_6$ was deposited there. The very low collection efficiency for plutonium (1.07%) in Run 4 should also be attributed to the $PuCd_6$ formation out of the cathode cadmium.

The electrotransport experiments were carried out also at the higher plutonium concentration in the molten salt (Runs 5–8). Before these tests, the concentration of plutonium in the molten salt was increased to 4.6 wt% by the procedure described in Section 2.4. Fig. 9 shows the change of the LCC potential in these tests. The overall tendency and the cathodic current density dependence of the cathode potential were similar to those seen in the preceding cases at the lower plutonium

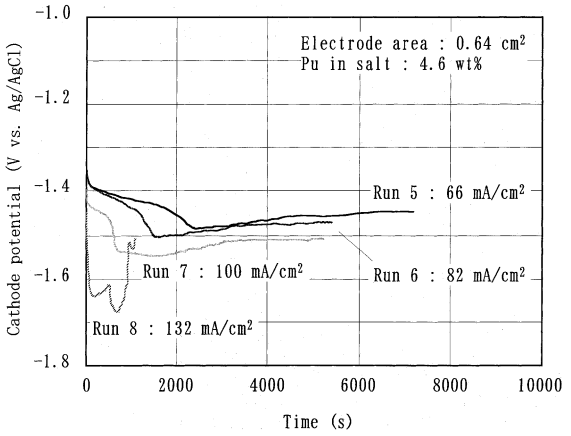

Fig. 9. Change of LCC potential in the Pu electrotransport tests (at the higher Pu concentration in molten salt).

concentrations. At the cathodic current density of up to 100 mA/cm^2, the cathode potential was kept higher than −1.6 V throughout the test and no growth of solid phase product was observed at the surface of the LCCs. In Run 8, where the highest cathodic current density (132 mA/cm^2) was applied, the cathode potential showed a rapid rise from −1.68 to −1.51 V. After cooling, small dendritic particles with metallic shine were observed in the molten salt phase just above the LCC. These results were also seen in Run 4 and indicate that $PuCd_6$ deposited out of the cathode cadmium due to the competitive reduction of lithium at the high cathodic current density.

3.2.2. Proper conditions for plutonium recovery with LCC

Fig. 10 summarizes the result of the electrotransport tests at various cathodic current densities and plutonium concentrations in the molten salt. The circles in this plot represent the conditions on which plutonium was smoothly collected into the LCC with the collection efficiency of almost 100%. The triangles denote the conditions on which the collection efficiency was decreased by the reduction of lithium and the reaction between the lithium and the ceramics parts. From these data, it is found that the maximum cathodic current density for successful plutonium collection with no-stirred LCC is proportional to the plutonium concentration in the molten salt as represented by the line in Fig. 10. This proportional relation indicates that the plutonium recovery rate was limited by transport of plutonium chloride to the surface of the LCC in the range of this study.

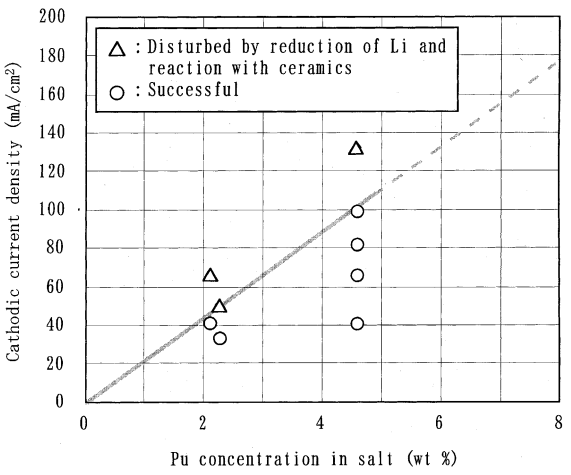

Fig. 10. Summary of the Pu electrotransport tests.

In practical electrorefining process, other factors should be taken into consideration. At higher plutonium concentration in the molten salt, the recovery rate can be controlled by the transport of reduced plutonium from the surface to the inside of the cathode as discussed in Section 3.1. On the other hand, larger cathodic current than shown in Fig. 10 can be expected in practical electrorefining equipment, because the LCC will be stirred to facilitate the transport of the actinide elements from the molten salt to the cathode cadmium.

However, an evaluation of plutonium recovery rate based on the experimental result, even at an early stage of development, is important because that kind of data is useful and necessary as a baseline for following tests in lager scale, investigations on the engineering factors, and design studies of whole pyrometallurgical processing plant. Then a rough estimation of plutonium recovery rate in practical scale electrorefining equipment was attempted as following by extrapolating the result from this study.

The sum of the concentrations of all actinides in the molten salt is planned to be adjusted to 2 mol% (about 8 wt%) in the practical operation of the electrorefining step [21]. In the LCC operation, the plutonium/uranium ratio in the molten salt will be set considerably high in order of avoid the formation of uranium dendrite. This ratio was assumed to be 7/1 in this estimation. The inner diameter of the practical scale LCC was assumed to be 30 cm. Because the slope of the rate limiting line in Fig. 10 was 22 mA/cm^2 wt% Pu, the reduction current of plutonium at one practical LCC can be evaluated as follows.

$$0.022\ (\mathrm{A/cm^2\ wt\%}) \times 7\ (\mathrm{wt\%}) \times 15^2\pi\ (\mathrm{cm^2}) = 109\ (\mathrm{A}).$$

This current is equivalent to a collection rate of 324 g of plutonium per hour. This performance is considered high enough as an initial condition for design of the practical electrorefiner and pyrometallurgical process.

3.2.3. Behavior of plutonium and americium in the LCC

The LCC ingot recovered after the electrotransport was analyzed by EPMA in order to evaluate the behavior and distribution of plutonium in the cathode. Fig. 11 is an SEM image of the intersection of the LCC ingot obtained in Run 2, where plutonium was collected into the cathode up to 7.75 wt% at cathodic current density of 41 mA/cm^2. There is a layer containing a crystallized phase in high density near the bottom of the LCC. Fig. 12 is a characteristic X-ray image of plutonium of this layer. It is clearly shown that the crystallized phase in this region contains a high concentration of plutonium and that only a small amount of plutonium exists in the bulk. The composition of the plutonium-rich phase was quantitatively analyzed in the following steps. X-ray counts for plutonium and cadmium from the LCC ingot sample were normalized by counts from pure plutonium and cadmium standard specimens. All these counts were corrected for background counts and dead time of the detector. Subsequently, the data were corrected by the ZAF method until it reached convergence. In the result, the mole ratio between cadmium and plutonium in the plutonium-rich phase was determined to be 6.08, indicating that the deposit was $PuCd_6$.

From these results, it seems most likely that plutonium reduced at the LCC beyond the solubility limit in liquid cadmium instantly forms $PuCd_6$ solid phase at the surface of the LCC and settled down to the bottom of the cathode. It is still possible, however, that the segregation of $PuCd_6$ was caused by the vertical temperature gradient in the LCC, because it was cooled very slowly at only a few centimeters above the top of the salt due to the safety requirement. Further tests are needed to elucidate the mechanism of $PuCd_6$ accumulation at the bottom of the LCC.

The PuO_2 used in this study contained about 2% of Am^{241} as described in 3.2. The exposure dose rate of γ-ray from Am^{241} in the LCC ingots was plotted as shown in Fig. 13 versus the total content of plutonium collected in the cathodes. The dose rate was measured at both the top and the bottom of the ingots by a GM survey meter placed outside of the glove box at a distance of about 1 mm from the ingots. These plots have a distinctive tendency. At the low concentrations of plutonium in the LCCs, the dose rate at either top or bottom of the ingots increased as the electrotransport proceeded. When the concentration of plutonium in the

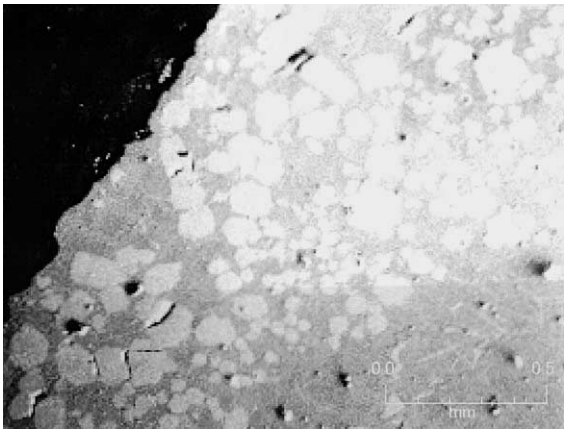

Fig. 11. SEM image of the LCC ingot shown in Fig. 7 (near the bottom).

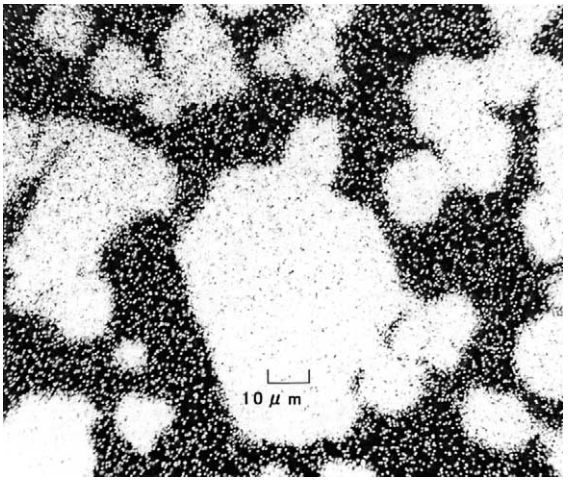

Fig. 12. Characteristic X-ray image of Pu at the bottom region of the LCC ingot.

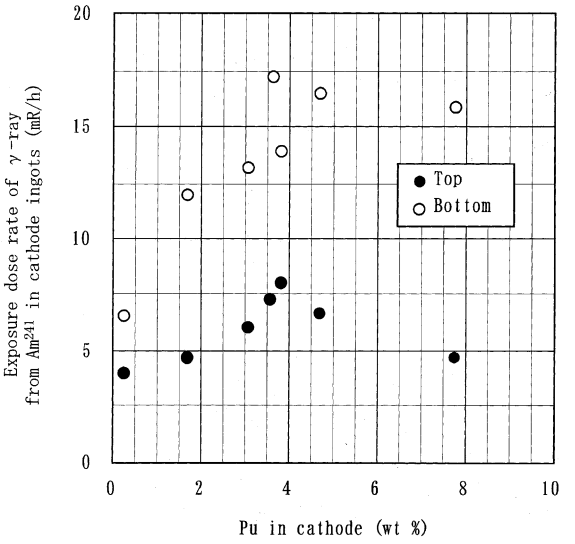

Fig. 13. Relation between the Pu concentration in the LCCs and γ-ray from the cathode ingots.

LCCs reached its solubility limit, however, the increase of the dose rate concurrently stopped. In our previous LCC study with uranium and lanthanide elements, similar behavior was observed (Fig. 14) [21]. While the concentration of uranium in the LCC increased linearly to the electricity, deposition of gadolinium and neodymium stopped before uranium saturation and their concentrations remained almost constant. Such behavior of americium and lanthanides can be explained by the consideration based on a local equilibrium model. Assuming that the electrode reactions of plutonium and americium at the LCC are reversible, that is, a local equilibrium relationship between the two elements at the cathode cadmium/molten salt interface described in equation in Fig. 15 is established at every moment. Activity of plutonium in the LCC increases with its concentration before it reaches solubility limit. After saturation, plutonium forms $PuCd_6$ solid phase and its activity in the LCC does not change although more plutonium would be collected. Under this condition, deposition of americium would be controlled so that the local equilibrium would be maintained.

It can be seen in Fig. 13 that the γ-ray exposure dose rate at the bottom of the ingot is always higher than that at the top. It means that americium exists at the bottom of the LCC at higher concentration than at the top. This result cannot be explained by the local equilibrium model. There may be two possible interpretations to the difference between the dose rates at the bottom and top. One is co-deposition of plutonium and americium in a form of a mixed intermetallic compound like $Pu_{1-x}Am_xCd_6$, and another is simply segregation at the bottom of the LCC in the course of cooling. In the former case, reduction of americium does not necessarily

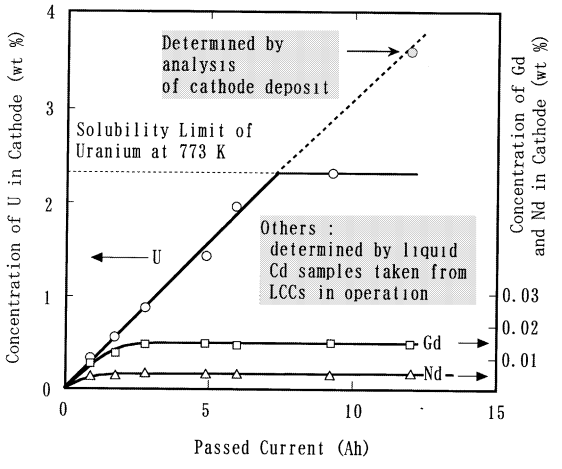

Fig. 14. Change of the LCC composition during the electrotransport experiment with uranium, gadolinium and neodymium [21].

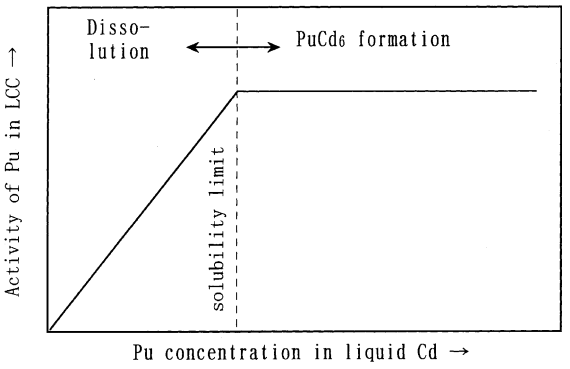

$$\frac{a\left(AmCl_{3\,salt/Cd}\right)}{a\left(Am_{\,Cd/salt}\right)} = K\frac{a\left(PuCl_{3\,salt/Cd}\right)}{a\left(Pu_{\,Cd/salt}\right)}$$

where

$a()$ represents activity of each species at the molten salt/LCC interface, and

$AmCl_{3\ salt/Cd}$	: $AmCl_3$ in molten salt
$Am_{\ Cd/salt}$	: Am in LCC
$PuCl_{3\ salt/Cd}$	: $PuCl_3$ in molten salt
$Pu_{\ Cd/salt}$	: Pu in LCC
K	: equilibrium constant

Fig. 15. Concept of the local equilibrium at the surface of the LCC.

be controlled by saturation of plutonium because the activity of americium in the LCC would not change by increase of $Pu_{1-x}Am_xCd_6$ solid phase. Although the behavior of americium in the LCC is very important data for the design of the electrorefining step and the pyrometallurgical process, no additional information was obtained in this study. For further understanding, the thermodynamic study on Pu–Am–Cd ternary system and the quantitative analysis of americium amount in the anode, the molten salt and the cathode will be needed.

4. Conclusions

1. From the CVs measured with the liquid cadmium electrode, it was found that reduction of plutonium occurs at −1.5 V (vs. Ag/AgCl) or higher at the LCC. This potential is about 0.2 V higher than that of a solid electrode in accordance with the low activity coefficient of plutonium in liquid cadmium.
2. Plutonium was collected into the no-stirred LCC without disturbance by solid phase formation at the surface. At plutonium concentration of 2.11 wt% in molten LiCl–KCl and cathodic current

density of 41 mA/cm^2, the collection efficiency of plutonium was nearly 100% and maximum plutonium loading into the LCC was 7.75 wt%. At the higher cathodic current densities, lithium metal was reduced and reacted with the ceramic LCC parts. The collection efficiency was decreased by $PuCd_6$ formation out of the LCC caused by those reactions.

3. The cathodic current density adequate for plutonium collection was proportional to the concentration of plutonium in the molten salt at the ratio of 22 mA/cm^2 wt% Pu in the range of this study. At plutonium concentration of 5.0 wt% in molten salt, cathodic current density of 100 mA/cm^2 was attained without any trouble such as solid deposit growth or descent of cathode potential indicating reduction of lithium. The plutonium collection rate in a practical scale electrorefiner was estimated to be 324 g/h for one LCC based on the assumption that the collection rate is proportional to the plutonium concentration in the molten salt and the surface area of the LCC. This performance is considered high enough as an initial condition for design of the practical electrorefiner and pyrometallurgical process.
4. It was considered that plutonium collected into the LCC after saturation formed intermetallic compound $PuCd_6$ and accumulated at the bottom of the LCC based on EPMA analysis of the LCC ingot. It is still possible, however, that segregation of $PuCd_6$ was caused by a vertical temperature gradient in the LCC in the course of the slow cooling process.
5. Increase of γ-ray count from Am^{241} in the LCC ingots stopped coincidently on saturation with plutonium. At present, this behavior can be reasonably explained with the local equilibrium model between plutonium and americium at the surface of the LCC. For further understanding, however, the thermodynamic study on Pu–Am–Cd ternary system and the quantitative analysis of americium will be needed.

Acknowledgements

This research was carried out under the joint program "Fundamental study on molten salt electrorefining" between the Japan Atomic Energy Research Institute (JAERI) and the Central Research Institute of Electric Power Industry (CRIEPI). The authors wish to thank Mr Shiozawa, JAERI, for chemical analysis of the samples. We would like to express special thanks to Mr Sasayama, JAERI. Without his expert knowledge on the apparatus design and the glove box work, this study would not have been successful. We also appreciate Dr Suzuki, JAERI, for continuing encouragement and helpful advice. Finally, we gratefully acknowledge the staff in the Plutonium Fuel Research Facility in the Oarai Research Establishment, JAERI for their warm support.

References

[1] Y.I. Chang, Nucl. Technol. 88 (1989) 129.
[2] T. Yokoo, M. Kawashima, Y. Tsuboi, in: Proceedings of the International Conference on the Physics of Reactors: Operation, Design and Computation (PHYSOR), Marseille, France, 1990, p. pIII-41.
[3] M. Tokiwai, T. Kobayashi, T. Koyama, M. Tsunashima, S. Horie, T. Matsuura, K. Yanagida, M. Shuto, in: Proceedings of the International Conference on Fast Reactors and Related Fuel Cycles (FR '91), Kyoto, Japan, vol. II, 1991, p. 12.7-1.
[4] T. Koyama, R. Fujita, M. Iizuka, Y. Sumida, Nucl. Technol. 110 (1995) 357.
[5] T. Koyama, K. Uozumi, M. Iizuka, Y. Sakamura and K. Kinoshita, Pyrometallurgical Data Book, CRIEPI Report T93033, 1995 (in Japanese).
[6] I. Johnson, M.G. Chasanov, R.M. Yonco, Trans. Metall. Soc. AIME 233 (1965) 1408.
[7] J. Roy, L. Grantham, D. Grimmett, S. Fusselman, C. Krueger, T. Storvick, T. Inoue, Y. Sakamura, N. Takahashi, J. Electrochem. Soc. 143 (1996) 2487.
[8] M. Kurata, A, Sasahara, T. Inoue, M. Betti, J. Babelot, J. Spirlet, L. Koch, in: Proceedings of the International Conference on Future Nuclear Systems (Global '97), Yokohama, Japan, vol. II, 1997, p. 1384.
[9] T. Yokoo, T. Ogata, K. Ohta, J. Nucl. Sci. Technol. 37 (2000) 636.
[10] Annual Technical Report for 1993, Chemical Technology Division, Argonne National Laboratory Report ANL-94/15, 1994, p. 89.
[11] Annual Technical Report for 1991, Chemical Technology Division, Argonne National Laboratory Report ANL-92/15, 1992, p. 120.
[12] Annual Technical Report for 1992, Chemical Technology Division, Argonne National Laboratory Report ANL-93/17, 1993, p. 112.
[13] Annual Technical Report for 1994, Chemical Technology Division, Argonne National Laboratory Report ANL-95/24, 1995, p. 86.
[14] T. Koyama, M. Iizuka, Y. Shoji, R. Fujita, H. Tanaka, T. Kobayashi, M. Tokiwai, J. Nucl. Sci. Technol. 34 (1997) 384.
[15] T. Koyama, M. Iizuka, N. Kondo, R. Fujita, H. Tanaka, J. Nucl. Mater. 247 (1997) 227.
[16] O. Shirai, T. Iwai, Y. Suzuki, Y. Sakamura, H. Tanaka, J. Alloys Compounds 271 (1998) 685.
[17] Y. Arai, S. Fukushima, K. Shiozawa, M. Handa, J. Nucl. Mater. 168 (1989) 280.
[18] For example A. Bard, L. Faulkner, Electrochemical Methods Fundamentals and Applications, Wiley, New York, 1980.

[19] T.B. Massalski (Ed.), Binary Alloy Phase Diagrams, ASM International, Materials Park, OH.
[20] M. Lewis, T. Johnson, J. Electrochem. Soc. 137 (1990) 1414.
[21] T. Koyama, M. Iizuka, H. Tanaka, in: Proceedings of the International Conference on Nuclear Engineering (ICONE-4), New Orleans, LA, 1996, p. 287.